Title
In vivo monoclonal antibody efficacy against SARS-CoV-2 variant strains

Journal
Nature, 596(7870)

ISSN
0028-0836

Authors
Chen, Rita E
Winkler, Emma S
Case, James Brett
et al.

Publication Date
2021-08-05

DOI
10.1038/s41586-021-03720-y

Peer reviewed

Published in final edited form as:

Nature. 2021 August ; 596(7870): 103–108. doi:10.1038/s41586-021-03720-y.

In vivo monoclonal antibody efficacy against SARS-CoV-2 variant strains

Rita E. Chen[#1,2], **Emma S. Winkler**[#1,2], **James Brett Case**[#1], **Ishmael D. Aziati**[1], **Traci L. Bricker**[1], **Astha Joshi**[1], **Tamarand L. Darling**[1], **Baoling Ying**[1], **John M. Errico**[2], **Swathi Shrihari**[1], **Laura A. VanBlargan**[1], **Xuping Xie**[3], **Pavlo Gilchuk**[4], **Seth J. Zost**[4], **Lindsay Droit**[5], **Zhuoming Liu**[5], **Spencer Stumpf**[5], **David Wang**[5], **Scott A. Handley**[2], **W. Blaine Stine Jr**[6], **Pei-Yong Shi**[3,7,8], **Meredith E. Davis-Gardner**[9], **Mehul S. Suthar**[9], **Miguel Garcia Knight**[10], **Raul Andino**[10], **Charles Y. Chiu**[11], **Ali H. Ellebedy**[2,16,17], **Daved H. Fremont**[2,5,12], **Sean P.J. Whelan**[5], **James E. Crowe Jr.**[4,13], **Lisa Purcell**[14], **Davide Corti**[15], **Adrianus C.M. Boon**[1,2,5], **Michael S. Diamond**[1,2,5,16,17,†]

[1]Department of Medicine, Washington University School of Medicine, St. Louis, MO. [2]Department of Pathology & Immunology, Washington University School of Medicine, St. Louis, MO. [3]Department of Biochemistry and Molecular Biology, University of Texas Medical Branch, Galveston TX [4]Vanderbilt Vaccine Center, Vanderbilt University Medical Center, Nashville, TN. [5]Department of Molecular Microbiology, Washington University School of Medicine, St. Louis, MO. [6]AbbVie Bioresearch Center, Worcester, Massachusetts [7]Departments of Microbiology and Immunology, University of Texas Medical Branch, Galveston TX [8]Sealy Institute for Vaccine Sciences, University of Texas Medical Branch, Galveston, TX [9]Center for Childhood Infections and Vaccines of Children's Healthcare of Atlanta, Department of Pediatrics, Emory Vaccine Center, Emory University School of Medicine, Atlanta, GA [10]Department of Microbiology and Immunology, University of California San Francisco, California, San Francisco, CA. [11]Departments

[†]**Corresponding author:** Michael S. Diamond, M.D., Ph.D., diamond@wusm.wustl.edu.

AUTHOR CONTRIBUTIONS

R.E.C. performed and analyzed neutralization assays. R.E.C., E.S.W., and J.B.C. performed mouse experiments. R.E.C., E.S.W., J.B.C., B.Y., and S.S. performed viral burden analyses. X.X. generated the recombinant SARS-CoV-2 viruses. R.E.C. and L.A.V. propagated and validated SARS-CoV-2 viruses. L.D., S.A.H., and D.W. performed deep sequencing analysis. I.D.A. and S.S. performed Sanger sequencing analyses. T.L.D., T.L.B., and A.C.M.B. performed the hamster studies. T.L.D. and A.J performed viral burden and inflammatory gene analysis. J.M.E. and D.H.F. performed structural analysis. Z.L. generated escape mutants. E.S.W. quantified serum antibody concentrations. J.B.C. and T.L.B. performed plaque assays. D.C., P.G., S.J.Z., W.B.S., J.E.C., A.H.E., W.B.S., and L.P. provided mAbs. M.S.S., M.E.D-G., P-Y.S., M.G.K., R.A., and C.Y.C. provided SARS-CoV-2 strains. P.Y.S., A.H.E., D.C., A.C.M.B. and M.S.D. obtained funding and supervised the research. R.E.C, E.S.W., J.B.C., and M.S.D. wrote the initial draft, with the other authors providing editorial comments.

COMPETING FINANCIAL INTERESTS

M.S.D. is a consultant for Inbios, Vir Biotechnology, Fortress Biotech, and Carnival Corporation, and on the Scientific Advisory Boards of Moderna and Immunome. The Diamond laboratory has received funding support in sponsored research agreements from Moderna, Vir Biotechnology, Kaleido, and Emergent BioSolutions. M.S.S. is on the Advisory Board of Moderna. J.E.C. has served as a consultant for Eli Lilly and Luna Biologics, is a member of the Scientific Advisory Boards of CompuVax and Meissa Vaccines and is Founder of IDBiologics. The Crowe laboratory has received sponsored research agreements from Takeda, AstraZeneca and IDBiologics. Vanderbilt University (J.E.C.) and Washington University (A.H.E., D.H.F., J.B.C., A.C.M.B., M.S.D.) have applied for patents related to antibodies in this paper. The Ellebedy laboratory has received funding support in sponsored research agreements from AbbVie Inc. and Emergent BioSolutions. The Boon laboratory has received funding support in sponsored research agreements from AI Therapeutics, GreenLight Biosciences, AbbVie, and Nano targeting & Therapy Biopharma. The Shi laboratory has received sponsored research agreements from Pfizer, Gilead, Merck, and IGM Sciences Inc. D.C. and L.P. are employees of Vir Biotechnology and may hold equity in Vir Biotechnology. L.P. is a former employee and may hold equity in Regeneron Pharmaceuticals. W.B.S. is an employee of AbbVie and may hold equity.

of Laboratory Medicine and Medicine, University of California San Francisco, San Francisco, CA. [12]Department of Biochemistry & Molecular Biophysics, Washington University School of Medicine, St. Louis, MO [13]Departments of Pediatrics and Pathology, Microbiology, and Immunology, Vanderbilt University Medical Center, Nashville, TN. [14]Vir Biotechnology, St. Louis, MO [15]Humabs BioMed SA, a subsidiary of Vir Biotechnology, Bellinzona, Switzerland. [16]Andrew M. and Jane M. Bursky Center for Human Immunology and Immunotherapy Programs, Washington University School of Medicine, Saint Louis, MO. [17]Center for Vaccines and Immunity to Microbial Pathogens, Washington University School of Medicine, Saint Louis, MO.

[#] These authors contributed equally to this work.

Abstract

Rapidly-emerging variants jeopardize antibody-based countermeasures against SARS-CoV-2. While cell culture experiments have demonstrated loss of potency of several anti-spike neutralizing antibodies against SARS-CoV-2 variant strains[1-3], the *in vivo* significance of these results remains uncertain. Using a panel of monoclonal antibodies (mAbs) corresponding to many in advanced clinical development by Vir Biotechnology, AbbVie, AstraZeneca, Regeneron, and Lilly, we report the impact on protection in animals against authentic SARS-CoV-2 variants including viruses with B.1.1.7, B.1.351, or B.1.1.28 spike genes. Although some individual mAbs showed reduced or abrogated neutralizing activity in cell culture against B.1.351, B.1.1.28, B.1.617.1, and B.1.526 viruses with E484 spike protein mutations, low prophylactic doses of mAb combinations protected against infection by many variants in K18-hACE2 transgenic mice, 129S2 immunocompetent mice, and hamsters without emergence of resistance. Exceptions were mAb LY-CoV555 and LY-CoV555/LY-CoV016 mono- and combination therapy, which lost all protective activity, and AbbVie 2B04/47D11, which showed partial loss of activity. When administered after infection as therapy, higher doses of several mAb cocktails protected *in vivo* against viruses with a B.1.351 spike gene. Thus, many, but not all, of the antibody products with Emergency Use Authorization (EUA) should retain substantial efficacy against the prevailing SARS-CoV-2 variant strains.

Severe acute respiratory syndrome coronavirus 2 (SARS-CoV-2) variant strains have emerged in the United Kingdom (B.1.1.7), South Africa (B.1.351), Brazil (B.1.1.28 [also called P.1]) and elsewhere containing substitutions in the N-terminal domain (NTD) and the receptor binding motif (RBM) of the RBD. Cell-based assays suggest that neutralization by many antibodies may be diminished against variants expressing spike mutations, especially at position E484[1-5]. However, the *in vivo* significance of this loss of mAb neutralizing activity remains uncertain, particularly for combination mAb therapies.

To evaluate the effects of SARS-CoV-2 strain variation on mAb protection, we assembled a panel of infectious SARS-CoV-2 strains with sequence substitutions in the spike gene (Fig 1a-b) including a B.1.1.7 isolate from the United Kingdom, a B.1.429 isolate from California, a B.1.617.1 isolate (India clade), and two B.1.526 isolates from New York. We also used a Washington SARS-CoV-2 strain with a D614G substitution (WA1/2020 D614G), a SARS-CoV-2 strain with N501Y and D614G substitutions (WA1/2020 N501Y/D614G),

and chimeric SARS-CoV-2 strains with B.1.351 (Wash-B.1.351) or B.1.1.28 (Wash-B.1.1.28) spike genes in the Washington strain background[1,6]. All viruses were propagated in Vero cells expressing transmembrane protease serine 2 (TMPRSS2) to prevent the emergence of mutations at or near the furin cleavage site in the spike protein that impact virulence[7]. All viruses were deep-sequenced to confirm the presence of expected mutations prior to use (Supplementary Table S1).

We first assessed the impact of SARS-CoV-2 spike variation on antibody neutralization (Fig 1c-d). We tested individual and cocktails of mAbs in clinical development that target the RBD including 2B04/47D11 (AbbVie), S309/S2E12 (Vir Biotechnology), COV2-2130/COV2-2196 (Vanderbilt University Medical Center with derivatives being evaluated by AstraZeneca), REGN10933/REGN10987 (synthesized based on casirivimab and imdevimab sequences from Regeneron), and LY-CoV555 (synthesized based on bamlanivimab sequences from Lilly). All individual mAbs tested efficiently neutralized the WA1/2020 D614G, WA1/2020 N501Y/D614G, and B.1.1.7 strains, and several mAbs (COV2-2130, COV2-2196, S309, S2E12, and 47D11) showed little change in potency against the Wash-B.1.351, Wash-B.1.1.28, B.1.429, and B.1.526 strains (Fig 1c-d). In comparison, REGN10987 or LY-CoV555 respectively showed a ~10-fold or complete loss in inhibitory activity against the B.1.429 and B.1.617.1 strains, which is consistent with studies identifying L452 and adjacent residues as interaction sites for these mAbs (Supplementary Table S2). Moreover, REGN10933, LY-CoV555, and 2B04 exhibited a substantial or complete loss of neutralizing activity against Wash-B.1.351, Wash-B.1.1.28, B.1.617.1, and B.1.526 (E484K) viruses that contain mutations at residue E484 (Fig 1c-d and Extended Data Fig 1), which corresponds with structural and mapping studies (Supplementary Table S2). Analysis of mAb cocktails showed that COV2-2130/COV2-2196, S309/S2E12, and REGN10933/REGN10987 neutralized all virus strains tested, with the latter combination retaining potency corresponding to the mAb with inhibitory activity in the cocktail for a given virus. While the 2B04/47D11 mAb combination efficiently neutralized WA1/2020 D614G, WA1/2020 N501Y/D614G, B.1.1.7, and B.1.429 strains, its activity against Wash-B.1.351, Wash-B.1.1.28, B.1.617.1, and B.1.526 (E484K) reflected the less potent 47D11 mAb component (EC_{50} of 384-2,187 ng/mL) (Fig 1c-d). Additional mutations in B.1.617.1 decreased the potency of the 2B04/47D11 combination further. In contrast, virtually all mAbs retained neutralizing potency against B.1.526 (S477N).

Prophylactic efficacy against variants

To evaluate the efficacy of the mAb combinations *in vivo*, we initially used K18-hACE2 mice in which human ACE2 expression is driven by the cytokeratin-18 gene promoter[8,9]. In prior studies, we established that low (2 mg/kg) doses of several anti-RBD neutralizing human mAbs provide a threshold of protection when administered as prophylaxis[10]. Accordingly, we gave K18-hACE2 mice a single 40 μg (~2 mg/kg total) dose of mAb combinations (2B04/47D11, S309/S2E12, COV2-2130/COV2-2196, or REGN10933/REGN10987) or LY-CoV555 as monotherapy by intraperitoneal injection one day prior to intranasal inoculation with SARS-CoV-2 (WA1/2020 N501Y/D614G, B.1.1.7, Wash-B.1.351 or Wash-B.1.1.28). For these *in vivo* studies, we used a recombinant version of WA1/2020 that encodes N501Y for direct comparison to B.1.1.7, Wash-B.1.351 or Wash-

B.1.1.28, all of which contain this residue. This substitution increases infection in mice[11,12] yet did not substantively impact neutralization of the mAbs we tested (Fig 1c).

Compared to a control human mAb, a single 40 μg prophylaxis dose of the anti-SARS-CoV-2 mAbs conferred substantial protection against WA1/2020 N501Y/D614G-induced weight loss and viral burden in the lungs, nasal washes, brain, spleen, and heart in the K18-hACE2 mice at 6 days post-infection (dpi) (Fig 2a-c, Extended Data Fig 2 and 3a). While all of the anti-SARS-CoV-2 mAb cocktails protected against weight loss caused by B.1.1.7, Wash-B.1.351 or Wash-B.1.1.28, LY-CoV555 monotherapy protected only against the B.1.1.7 strain (Fig 2d, g, and j). Some of the antibodies provided less virological protection against the B.1.1.7, Wash-B.1.351 or Wash-B.1.1.28 strains in specific tissues. Whereas all mAb groups protected against B.1.1.7 infection in the lung, 2B04/47D11 and LY-CoV555 failed to perform as well in nasal washes, and LY-CoV555 showed reduced protection in the brain (Fig 2e-f, h-i, k-l, Extended Data Fig 2). Sanger sequencing analysis of the RBD region of viral RNA of brain, nasal wash, and lung samples from animals treated with these mAbs did not show evidence of neutralization escape (Supplementary Table S3). 2B04/47D11 and LY-CoV555-treated animals also showed greater virus breakthrough than the other tested antibodies when challenged with Wash-B.1.351 or Wash-B.1.1.28 viruses: 2B04/47D11 reduced viral burden in the lungs, nasal washes, and brain much less efficiently than other mAb cocktails, and LY-CoV555 mAb treatment conferred virtually no protection in any tissue analyzed (Fig 2h-i, k-l and Extended Data Figs 2 and 3b). Compared to the COV2-2130/COV2-2196 and S309/S2E12 combinations, REGN10933/REGN10987 also showed less ability to reduce viral RNA levels in nasal washes of mice infected with Wash-B.1.351 or Wash-B.1.1.28 viruses. To confirm that our findings with Wash-B.1.351 are similar to a *bona fide* B.1.351 strain, we tested mAbs from each cocktail for neutralization and the COV2-2130/COV2-2196 cocktail for protection in K18-hACE2 mice. Equivalent levels of neutralization and viral burden reduction were seen with B.1.351 and Wash-B.1.351 viruses (Extended Data Fig 4).

To evaluate further the extent of protection conferred by the different mAb groups against the SARS-CoV-2 variant viruses, we measured pro-inflammatory cytokine and chemokines in lung homogenates harvested at 6 dpi (Extended Data Figs 5 and 6). This analysis showed a strong correspondence with viral RNA levels in the lung: (a) compared to the control mAb, S309/S2E12, COV2-2130/COV2-2196, and REGN10933/REGN10987 combinations showed markedly reduced levels of pro-inflammatory cytokines and chemokines (G-CSF, IFN-γ, IL-6, CXCL10, LIF, CCL2, CXCL9, CCL3, and CCL4) after infection with WA1/2020 N501Y/D614G, B.1.1.7, Wash-B.1.351 or Wash-B.1.1.28; (b) prophylaxis with 2B04/47D11 or LY-CoV555 resulted in reduced inflammatory cytokine and chemokine levels in mice infected with WA1/2020 N501Y/D614G and B.1.1.7, with less improvement in animals infected with Wash-B.1.351 or Wash-B.1.1.28.

Given that a 40 μg dose of S309/S2E12, COV2-2130/COV2-2196, and REGN10933/REGN10987 combinations prevented infection and inflammation caused by the different SARS-CoV-2 strains, we tested a ten-fold lower 4 μg dose (~0.2 mg/kg) to assess for possible differences in protection. Prophylaxis with COV2-2130/COV2-2196, S309/S2E12, REGN10933/REGN10987, or 2B04/47D11 protected K18-hACE2 mice against weight loss

caused by all four viruses (Extended Data Fig 7a-d). Whereas the COV2-2130/COV2-2196, S309/S2E12, and REGN10933/REGN10987 mAb combinations reduced viral RNA levels in the lung at 6 dpi in K18-hACE2 mice infected with WA1/2020 N501Y/D614G, B.1.1.7, Wash-B.1.351, or Wash-B.1.1.28, the 2B04/47D11 treatment conferred protection against B.1.1.7 and WA1/2020 N501Y/D614G but not against Wash-B.1.351 or Wash-B.1.1.28 viruses at this lower dose (Extended Data Fig 7e-h). In comparison, in nasal washes, all four mAb cocktails resulted in relatively similar reductions in viral RNA levels at 6 dpi of animals inoculated with WA1/2020 N501Y/D614G, B.1.1.7, Wash-B.1.351 or Wash-B.1.1.28 (Extended Data Fig 7i-l). Even at this low treatment dose, with the exception of some substantive breakthrough events (>6 log 10 copies of N/mg: COV2-2130/COV2-2196 [2 of 24 mice]; S309/S2E12 [6 of 24 mice]; REGN10933/REGN10987 [1 of 24 mice]; and 2B04/47D11 [6 of 24 mice]), the mAb combinations generally prevented infection of the brain (Extended Data Fig 7m-p and Supplementary Table S3). Overall, the neutralization activity of mAbs *in vitro* against SARS-CoV-2 variants correlated with lung viral burden after prophylactic administration (Extended Data Fig 8).

As an alternative model for evaluating mAb efficacy, we tested immunocompetent, inbred 129S2 mice, which are permissive to infection by SARS-CoV-2 strains encoding an N501Y substitution without hACE2 expression[11,12]; presumably, the N501Y adaptive mutation enables engagement of murine (m)ACE2. We administered a single 40 μg (~2 mg/kg) dose of mAb cocktails (COV2-2130/COV2-2196, S309/S2E12, or REGN10933/REGN10987) or a control mAb via intraperitoneal injection one day prior to intranasal inoculation with 10^3 FFU of WA1/2020 N501Y/D614G, Wash-B.1.351, or Wash-B.1.1.28, and 10^5 FFU of B.1.1.7 (Extended Data Fig 9). A higher inoculating dose of B.1.1.7 was required to obtain equivalent levels of viral RNA in the lung compared to the other three viruses. At 3 dpi, we harvested tissues for viral burden analyses; at this time point, reproducible weight loss was not observed. All three mAb cocktails tested (COV2-2130/COV2-2196, S309/S2E12, and REGN10933/REGN10987) protected 129S2 mice against infection in the lung by all SARS-CoV-2 strains (Extended Data Fig 9a-d); despite some variability, we observed a trend toward less complete protection in animals infected with Wash-B.1.351 and Wash-B.1.1.28 strains (Extended Data Fig 3c-f). When we evaluated the nasal washes, reductions in viral RNA levels were diminished with the Wash-B.1.351 virus, especially for the COV2-2130/COV2-2196 and REGN10933/REGN10987 combinations (Extended Data Fig 9e-h). Sequencing analysis of lung samples from the infected 129S2 mice also did not reveal evidence of acquisition of mutations in the RBD (Supplementary Table S3).

The immunocompetent Syrian golden hamster also has been used to evaluate mAb activity against SARS-CoV-2 infection[13,14]. We used this animal model to assess independently the inhibitory activity and possible emergence of resistance of one of the mAb combinations (COV2-2130/COV2-2196) against viruses containing the B.1.351 spike protein. One day prior to intranasal inoculation with 5 x 10^5 FFU of Wash-B.1.351 or WA1/2020 D614G, we treated hamsters with a single 800 μg (~10 mg/kg) or 320 μg (~4 mg/kg) dose of the COV2-2130/COV2-2196 cocktail or isotype control mAb by intraperitoneal injection (Extended Data Fig 10). Weights were followed for 4 days, and tissues were harvested for virological and cytokine analysis. At the 800 μg mAb cocktail dose, hamsters treated with COV2-2130/COV2-2196 and infected with WA1/2020 D614G or Wash-B.1.351 showed

protection against weight loss and reduced viral burden levels in the lungs but not nasal swabs compared to the isotype control mAb (Extended Data Fig 10a-d). Correspondingly, RT-qPCR analysis of a previously described set of cytokines and inflammatory genes[10] showed reduced mRNA expression in the lungs of hamsters treated with COV2-2130/COV2-2196 (Extended Data Fig 10e-h). Consensus sequencing of the RBD region of viral RNA samples from the lungs of hamsters treated with COV2-2130/COV2-2196 did not show evidence of mutation or escape (Supplementary Table S3). When the lower 320 μg dose of COV2-2130/COV2-2196 was administered, we observed a trend toward protection against weight loss in hamsters infected with WA1/2020 D614G and Wash-B.1.351. Consistent with a partially protective phenotype, hamsters treated with the lower 320 μg dose of COV2-2130/COV2-2196 and inoculated with either WA1/2020 D614G and Wash-B.1.351 showed a trend towards reduced viral RNA in the lungs at 4 dpi and markedly diminished (~10^4 to 10^5-fold) levels of infectious virus as determined by plaque assay (Extended Data Fig 10j-k). The reduction in lung viral load conferred by the lower dose COV2-2130/COV2-2196 corresponded with diminished inflammatory gene expression after infection with either WA1/2020 D614G or Wash-B.1.351 (Extended Data Fig 10m-p). In contrast to the protection seen in the lung, differences in viral RNA were not observed in nasal washes between COV2-2130/COV2-2196 and isotype control mAb-treated animals regardless of the infecting strain (Extended Data Fig 10l). Sequencing of the RBD of viral RNA from the lungs of COV2-2130/COV2-2196 or isotype mAb-treated hamsters also did not detect evidence of escape mutation selection after infection (Supplementary Table S3). Overall, these studies in hamsters with near threshold dosing of the COV2-2130/COV2-2196 mAb cocktail establish protection and an absence of rapid escape against SARS-CoV-2 containing spike proteins from historical or variant strains.

Therapeutic efficacy against variants

As mAbs are being developed clinically as therapeutics, we assessed their post-exposure efficacy against the SARS-CoV-2 strain expressing the B.1.351 spike protein using K18-hACE2 mice. We administered a single, higher 200 μg (~10 mg/kg) dose of COV2-2130/COV2-2196, S309/S2E12, REGN10933/REGN10987, or 2B04/47D11 by intraperitoneal injection one day after inoculation with WA1/2020 N501Y/D614G or Wash-B.1.351 (Fig 3). Compared to the control mAb-treated animals, which lost at least 15% of their starting weight over the 6 days of the experiment, each of these mAb cocktails prevented weight loss induced by WA1/2020 N501Y/D614G or Wash-B.1.351 infection (Fig 3a and d). Histopathological analysis of lung sections from control mAb-treated animals showed interstitial edema, immune cell infiltration, and collapsed alveolar spaces, consistent with the inflammation induced by Wash-B.1.351 SARS-CoV-2 infection (Extended Data Fig 11). In contrast, COV2-2130/COV2-2196, S309/S2E12, REGN10933/REGN10987, and 2B04/47D11 treated animals showed reduced or minimal lung pathology. COV2-2130/COV2-2196, S309/S2E12, and REGN10933/REGN10987 mAb cocktail treatments resulted in reduced infectious virus and viral RNA levels in lung homogenates, and viral RNA levels in nasal washes and brain homogenates from animals infected with either WA1/2020 N501Y/D614G or Wash-B.1.351 (Fig 3b-c, e-f and Extended Data Fig 3g-h, Extended Data Fig 12). In comparison, while the 2B04/47D11 mAb cocktail reduced viral RNA levels in

the lungs, it showed less protection in the nasal washes of WA1/2020 N501Y/D614G and Wash-B.1.351 infected mice. Although neutralizing capacity correlated with lung viral burden when mAbs were administered as prophylaxis, this association was less direct when mAbs were given in the post-exposure setting (Extended Data Figure 8). This result was not entirely unexpected, as effector functions of some mAbs are required for optimal activity when given as post-exposure therapy[10,15]. Indeed, recent studies with influenza and SARS-CoV-2 neutralizing antibodies suggest that Fc engagement mitigates inflammation, improves respiratory mechanics, and promotes viral clearance in the lung[10,16].

With the emergence of several SARS-CoV-2 variants, it remains uncertain whether vaccines and antibody-based therapies will lose efficacy[17]. Cell-culture based studies have shown that several of the mutations in variant strains, especially those at positions 452 and 484, result in reduced neutralization by antibodies derived from infected or vaccinated individuals[1-3,18,19]. Here we evaluated antibodies forming the basis of five mAb therapies in clinical development for *in vivo* efficacy against infection by SARS-CoV-2 variants. Monotherapy with LY-CoV555, an antibody corresponding to bamlanivimab[20], showed complete neutralization escape in cell culture and failed to confer protection against viruses containing E484 substitutions. In contrast, all cocktails of two neutralizing mAbs conferred protection to varying degrees even if one of the constituent mAbs showed reduced activity due to resistance. Moreover, the higher doses of mAbs used in patients (*e.g.*, ~ 35 mg/kg for casirivimab and imdevimab [REGN mAbs]) could compensate for loss in neutralization potency. Generally, in mice and hamsters, mAb-mediated protection was better in the lung than in nasal washes, possibly because IgG levels in the respiratory mucosa are lower than in plasma[21,22].

Combination therapy with multiple mAbs in our study was protective in mice and hamsters against variant strains, highlighting the importance of using multiple mAbs recognizing distinct epitopes rather than monotherapy to control SARS-CoV-2 infection. Indeed, the EUA for bamlanivimab (LY-CoV555) as monotherapy was revoked, since the antibody does not reduce SARS-CoV-2 infection of several variants of concern[2,23,24]; instead, a combination of bamlanivimab (LY-CoV555) and etesevimab (LY-CoV016) is recommended even though strains containing E484 and K417 mutations (*e.g.*, B.1.351, B.1.1.28, B.1.617.1, and B.1.526) likely will have resistance to both mAb components ([2,25] and Extended Data Fig 13). Indeed, in K18-hACE2 mice, we found that LY-CoV555/LY-CoV016 had therapeutic activity against WA1/2020 N501Y/D614G (Fig 3a-c) but not against Wash-B.1.351 (Fig 3d-f). This failure of protection occurred because both mAbs in the cocktail lost neutralizing activity. Other cocktails may fair better against variants of concern as long as one of the mAbs in each pair retains substantial inhibitory activity. Beyond a loss of potency against already circulating resistant variants, antibody monotherapy can be compromised within an individual by rapid selection of escape mutations. Consistent with this idea, in other animal experiments with SARS-CoV-2, we observed emergence of resistance against antibody monotherapy, resulting in the accumulation of mutations at RBD residues 476, 477, 484, and 487 ([26] and M. Diamond, unpublished data). Remarkably, and despite amplifying sequences from 99 brain, nasal wash, and lung samples from mice and hamsters treated with the different mAb combinations, we did not detect a single escape mutant. Combination mAb treatment may

prevent escape through synergistic interactions *in vivo* or by driving selection of mutants with compromised fitness.

At the lower doses of mAbs tested, we observed some differences in mAb cocktail efficacy between rodent models, which could be due to host variation, viral variation, or small differences in antibody levels. For example, mutations in the RBD can affect mAb binding as well as ACE2 binding[27]. Mutation at position 501 of the spike is of particular interest, since it enables mouse adaptation[11,12] and is present in several variants of concern. The N501Y change associated with infection of conventional laboratory mice could facilitate virus engagement with murine ACE2 or possibly other putative receptors. Beyond this, polymorphisms in or differences of expression of host receptors on key target cells also could impact SARS-CoV-2 infection in different hosts and the inhibitory effects of neutralizing antibodies. This complexity of antibody-spike protein-receptor interactions likely explains some of the variation in protection between K18-hACE2 mice, 129S2 mice, and hamsters. Alternatively, the pharmacokinetics of human antibodies could vary between animals and affect efficacy. We observed small differences in serum antibody levels in the context of viral challenge that could impact relative protection (Supplementary Table S4).

Studies with pseudoviruses and authentic SARS-CoV-2 containing variant substitutions suggested that adjustments to therapeutic antibody regimens might be necessary[1,2,28-30]. Although our studies with variant strains *in vivo* suggest this conclusion likely holds for mAb monotherapy, four different mAb combinations performed well even when a virus was fully resistant to one mAb component. Thus, our results suggest that, as described with the historical WA1/2020 strain[31], many but not all combination therapies with neutralizing mAbs should retain efficacy against emerging SARS-CoV-2 variants.

METHODS

Cells.

Vero-TMPRSS2[33] and Vero-hACE2-TMPRRS2[1] cells were cultured at 37°C in Dulbecco's Modified Eagle medium (DMEM) supplemented with 10% fetal bovine serum (FBS), 10 mM HEPES pH 7.3, 1 mM sodium pyruvate, 1× non-essential amino acids, and 100 U/ml of penicillin–streptomycin. Vero-TMPRSS2 cells were supplemented with 5 μg/mL of blasticidin. Vero-hACE2-TMPRSS2 cells were supplemented with 10 μg/mL of puromycin. All cells routinely tested negative for mycoplasma using a PCR-based assay.

Viruses.

The WA1/2020 recombinant strain with substitutions (D614G or N501Y/D614G) were obtained from an infectious cDNA clone of the 2019n-CoV/USA_WA1/2020 strain as described previously[34]. The B.1.351 and B.1.1.28 variant spike genes were introduced into the WA1/2020 backbone as described previously to create chimeric SARS-CoV-2[1]. The B.1.1.7, B.1.429, B.1.351, and B.1.526 (S477N or E484K variant) isolates were obtained from nasopharyngeal isolates. The B.1.617.1 variant was plaque purified from a midturbinate nasal swab and passaged twice on Vero-TMPRSS2 cells as described[35]. All viruses were passaged once in Vero-TMPRSS2 cells and subjected to next-generation

sequencing as described previously[1] to confirm the introduction and stability of substitutions (Supplementary Table S1). Substitutions for each variant were as follows: **B.1.1.7**: 69-70 deletion, 144-145 deletion, N501Y, A570D, D614G, P681H, T716I, S982A, and D1118H; **B.1.351**: D80A, T95I, D215G, 242-244 deletion, K417N, E484K, N501Y, D614G, and A701V; **B.1.1.28**: L18F, T20N, P26S, D138Y, R190S, K417T, E484K, N501Y, D614G, H655Y, and T1027I; **B.1.429**: S13I, W152C, L452R, and D614G; **B.1.617.1**: G142D, E154K, L452R, E484Q, D614G, P681R, Q1071H, and H1101D; and **B.1.526** (S477N or E484K variant): L5F, T95I, D253G, S477N, E484K, D614G, and A701V or Q957R. All virus experiments were performed in an approved biosafety level 3 (BSL-3) facility.

Monoclonal antibody purification.

The mAbs studied in this paper (COV2-2196, COV2-2130, S309, S2E12, 2B04, 47D11, REGN10933, REGN10987, LY-CoV555, and LY-CoV016) have been described previously[31,36-42]. COV2-2196 and COV2-2130 mAbs were produced after transient transfection using the Gibco ExpiCHO Expression System (ThermoFisher Scientific) following the manufacturer's protocol. Culture supernatants were purified using HiTrap MabSelect SuRe columns (Cytiva, formerly GE Healthcare Life Sciences) on an AKTA Pure chromatographer (GE Healthcare Life Sciences). Purified mAbs were buffer-exchanged into PBS, concentrated using Amicon Ultra-4 50-kDa centrifugal filter units (Millipore Sigma) and stored at −80 °C until use. Purified mAbs were tested for endotoxin levels (found to be less than 30 EU per mg IgG). Endotoxin testing was performed using the PTS201F cartridge (Charles River), with a sensitivity range from 10 to 0.1 EU per mL, and an Endosafe Nexgen-MCS instrument (Charles River). S309, S2E12, REGN10933, REGN10987, LY-CoV016, and LY-CoV555 mAb proteins were produced in CHOEXPI cells and affinity purified using HiTrap Protein A columns (GE Healthcare, HiTrap mAb select Xtra #28-4082-61). Purified mAbs were suspended into 20 mM histidine, 8% sucrose, pH 6.0. The final products were sterilized by filtration through 0.22μm filters and stored at 4°C.

Mouse experiments.

Animal studies were carried out in accordance with the recommendations in the Guide for the Care and Use of Laboratory Animals of the National Institutes of Health. The protocols were approved by the Institutional Animal Care and Use Committee at the Washington University School of Medicine (assurance number A3381–01). Virus inoculations were performed under anesthesia that was induced and maintained with ketamine hydrochloride and xylazine, and all efforts were made to minimize animal suffering.

Heterozygous K18-hACE2 C57BL/6J mice (strain: 2B6.Cg-Tg(K18-ACE2)2Prlmn/J) and 129 mice (strain: 129S2/SvPasCrl) were obtained from The Jackson Laboratory and Charles River Laboratories, respectively. Animals were housed in groups and fed standard chow diets. Six- to ten-week-old mice of both sexes were administered 10^3 or 10^5 FFU of the respective SARS-CoV-2 strain by intranasal administration. *In vivo* studies were not blinded, and mice were randomly assigned to treatment groups. No sample-size calculations were performed to power each study. Instead, sample sizes were determined based on prior *in vivo* virus challenge experiments.

For antibody prophylaxis and therapeutic experiments, animals were administered the indicated mAb dose by intraperitoneal injection one day before or after intranasal inoculation with the indicated SARS-CoV-2 strain.

Hamster experiments.

Six-month-old male Syrian hamsters were purchased from Charles River Laboratories and housed in microisolator units. All hamsters were allowed free access to food and water and cared for under United States Department of Agriculture (USDA) guidelines for laboratory animals. Hamsters were administered by intraperitoneal injection mAbs COV2-2130 + COV2-2196 or isotype control (4 or 10 mg/kg depending on the experiment). One day later, hamsters were given 5 x 10^5 FFU of indicated SARS-CoV-2 strain by the intranasal route in a final volume of 100 μL. All hamsters were monitored for body weight loss until humanely euthanized at 4 dpi. Nasal swabs were collected 3 dpi. All procedures were approved by the Washington University School of Medicine (assurance number A3381–01). Virus inoculations and antibody transfers were performed under anesthesia that was induced and maintained with 5% isoflurane. All efforts were made to minimize animal suffering.

Focus reduction neutralization test.

Serial dilutions of mAbs (starting at 10 μg/mL dilution) were incubated with 10^2 focus-forming units (FFU) of different strains or variants of SARS-CoV-2 for 1 h at 37°C. Antibody-virus complexes were added to Vero-TMPRSS2 cell monolayers in 96-well plates and incubated at 37°C for 1 h. Subsequently, cells were overlaid with 1% (w/v) methylcellulose in MEM. Plates were harvested 30 h later by removing overlays and fixed with 4% PFA in PBS for 20 min at room temperature. Plates were washed and sequentially incubated with an oligoclonal pool of SARS2-2, SARS2-11, SARS2-16, SARS2-31, SARS2-38, SARS2-57, and SARS2-71[43] anti-S antibodies and HRP-conjugated goat anti-mouse IgG (Sigma, 12-349) in PBS supplemented with 0.1% saponin and 0.1% bovine serum albumin. SARS-CoV-2-infected cell foci were visualized using TrueBlue peroxidase substrate (KPL) and quantitated on an ImmunoSpot microanalyzer (Cellular Technologies).

Measurement of viral burden.

Tissues were weighed and homogenized with zirconia beads in a MagNA Lyser instrument (Roche Life Science) in 1000 μL of DMEM medium supplemented with 2% heat-inactivated FBS. Tissue homogenates were clarified by centrifugation at 10,000 rpm for 5 min and stored at −80°C. RNA was extracted using the MagMax mirVana Total RNA isolation kit (Thermo Fisher Scientific) on the Kingfisher Flex extraction robot (Thermo Fisher Scientific). RNA was reverse transcribed and amplified using the TaqMan RNA-to-CT 1-Step Kit (Thermo Fisher Scientific). Reverse transcription was carried out at 48°C for 15 min followed by 2 min at 95°C. Amplification was accomplished over 50 cycles as follows: 95°C for 15 s and 60°C for 1 min. Copies of SARS-CoV-2 N gene RNA in samples were determined using a previously published assay[44]. Briefly, a TaqMan assay was designed to target a highly conserved region of the N gene (Forward primer: ATGCTGCAATCGTGCTACAA; Reverse primer: GACTGCCGCCTCTGCTC; Probe: /56-FAM/TCAAGGAAC/ZEN/AACATTGCCAA/3IABkFQ/). This region was included in an RNA standard to allow for copy number determination down to 10 copies per reaction. The

reaction mixture contained final concentrations of primers and probe of 500 and 100 nM, respectively.

Plaque assay.

Vero-TMPRSS2-hACE2 cells were seeded at a density of 1×10^5 cells per well in 24-well tissue culture plates. The following day, medium was removed and replaced with 200 μL of material to be titrated diluted serially in DMEM supplemented with 2% FBS. One hour later, 1 mL of methylcellulose overlay was added. Plates were incubated for 72 h, then fixed with 4% paraformaldehyde (final concentration) in PBS for 20 min. Plates were stained with 0.05% (w/v) crystal violet in 20% methanol and washed twice with distilled, deionized water.

Cytokine and chemokine protein measurements.

Lung homogenates were incubated with Triton-X-100 (1% final concentration) for 1 h at room temperature to inactivate SARS-CoV-2. Homogenates then were analyzed for cytokines and chemokines by Eve Technologies Corporation (Calgary, AB, Canada) using their Mouse Cytokine Array / Chemokine Array 31-Plex (MD31) platform.

Lung histology.

Animals were euthanized before harvest and fixation of tissues. Lungs were inflated with ~2 mL of 10% neutral buffered formalin using a 3-mL syringe and catheter inserted into the trachea and kept in fixative for 7 days. Tissues were embedded in paraffin, and sections were stained with hematoxylin and eosin. Images were captured using the Nanozoomer (Hamamatsu) at the Alafi Neuroimaging Core at Washington University.

Data availability.

All data supporting the findings of this study are available within the paper and are available from the corresponding author upon request.

Statistical analysis.

All statistical tests were performed as described in the indicated figure legends using Prism 8.0. Statistical significance was determined using an ordinary one-way ANOVA with Dunnett’s post-test when comparing three or more groups. The number of independent experiments used are indicated in the relevant Figure legends.

Extended Data

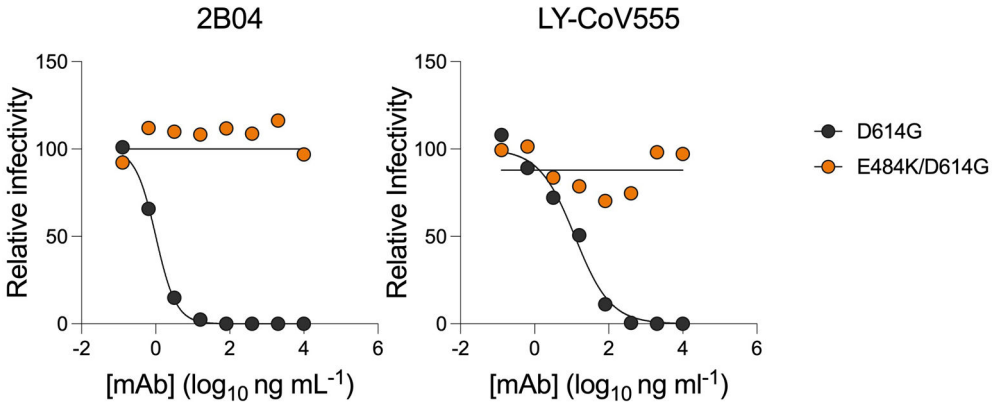

Extended Data Figure 1. Neutralization curves with mAbs and variant SARS-CoV-2 strains.
Anti-SARS-CoV-2 human mAbs were tested for inhibition of infection of the indicated viruses on Vero-TMPRSS2 cells using a focus reduction neutralization test. One representative experiment of two performed in duplicate is shown.

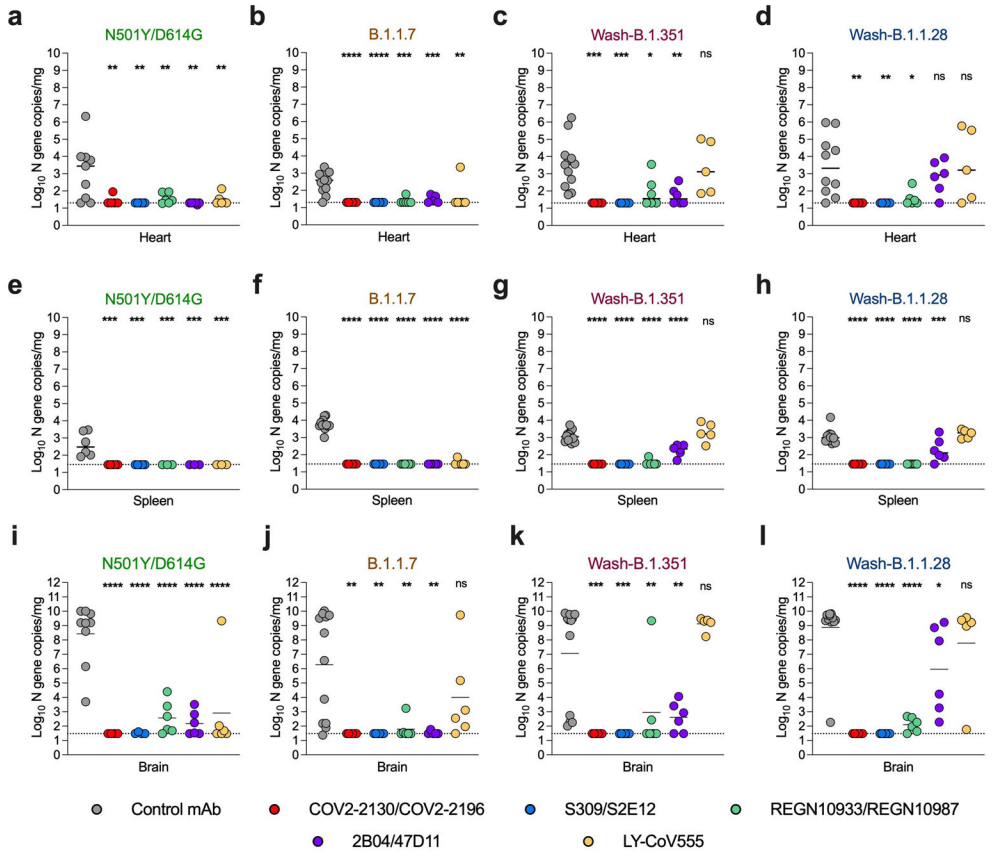

Extended Data Figure 2. SARS-CoV-2 variant infection after antibody prophylaxis of K18-hACE2 mice.
(**a-l**) 8-10-week-old female and male K18-hACE2 transgenic mice received 40 μg of the indicated mAb treatment by intraperitoneal injection one day before intranasal challenge

with 10^3 FFU of the indicated SARS-CoV-2 strain. At 6 dpi, viral RNA levels in the heart (**a-d**), spleen (**e-h**), and brain (**i-l**) were measured (line indicates median; in order left to right n = 9, 5, 5, 6, 6, 6 (**a**); n = 12, 6, 6, 6, 5, 6 (**b, c, f, g, j, k**); n = 10, 6, 6, 6, 6, 5 (**d, h**); n = 6, 5, 5, 3, 3, 3 (**e**); n = 9, 4, 4, 6, 6, 6 (**i**); n = 11, 6, 6, 6, 6, 5 (**l**) mice per group, two experiments; one-way ANOVA with Dunnett's test with comparison to control mAb: ns, not significant, **** $P < 0.0001$; in order left to right ** $P = 0.0066$, 0.0032, 0.0080, 0.0016, 0.0052 (**a**); *** $P = 0.0002$, ** $P = 0.0017$, 0.0052 (**b**); *** $P = 0.0004$, 0.0004, * $P = 0.0140$, ** $P = 0.0043$ (**c**); ** $P = 0.0080$, 0.0080, * $P = 0.0226$ (**d**); *** $P = 0.0001$, 0.0001, 0.0008, 0.0008, 0.0008 (**e**); *** $P = 0.0008$ (**h**); ** $P = 0.0014$, 0.0014, 0.0029, 0.0032 (**j**); *** $P = 0.0002$, 0.0002, ** $P = 0.0061$, 0.0028 (**k**); * $P = 0.0371$ (**l**)). Dotted line indicates the limit of detection of the assay.

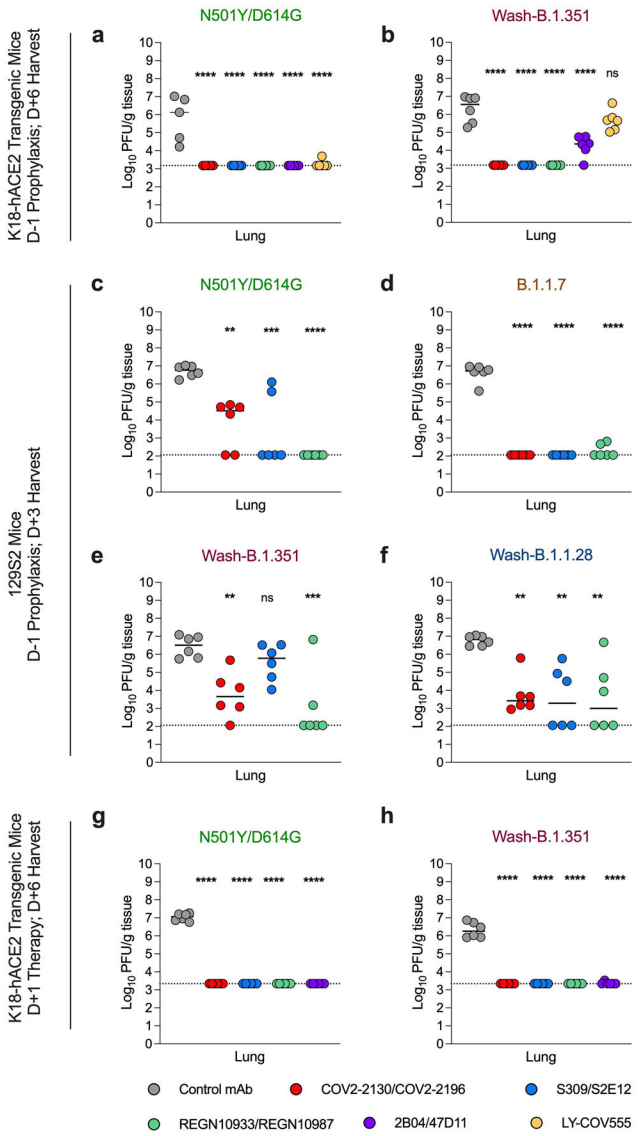

Extended Data Figure 3. Reduced infectious virus in the lungs of antibody-treated mice.

(**a-b**) 8-10-week-old female and male K18-hACE2 transgenic mice received 40 μg (~2 mg/kg) of the indicated mAb treatment by intraperitoneal injection one day before intranasal inoculation with 10^3 FFU of the indicated SARS-CoV-2 strain. Tissues were collected at 6 dpi. (**c-f**) 6-7-week-old female and male immunocompetent 129S2 mice received 40 μg (~ 2 mg/kg) of the indicated mAb treatment by intraperitoneal injection one day before intranasal inoculation with 10^3 FFU of WA1/2020 N501Y/D614G, Wash-B.1.351, or Wash-B.1.1.28 and 10^5 FFU of B.1.1.7. Tissues were collected at 3 dpi. (**g-h**) 8-10-week-old female and male K18-hACE2 transgenic mice were administered 10^3 FFU of the indicated SARS-CoV-2 strain by intranasal inoculation. One day later, animals received 200 μg (~10 mg/kg) of the indicated mAb treatment by intraperitoneal injection. Tissues were collected at 6 dpi. For all panels, infectious virus in lung homogenates was determined by plaque assay using Vero-TMPRSS2-hACE2 cells (line indicates median; in order left to right n = 5, 5, 5, 6, 6, 6 (**a**); n = 6, 6, 6, 6, 6, 6 (**b-h**) mice per group, one-way ANOVA with Dunnett's test with comparison to control mAb: ns, not significant, **** $P < 0.0001$; ** $P = 0.0012$, *** $P = 0.0003$ (**c**); ** $P = 0.0048$, *** $P = 0.0005$ (**e**); ** $P = 0.0031$, 0.0019, 0.0020 (**f** left to right)). Dotted lines indicate the limit of detection of the assay.

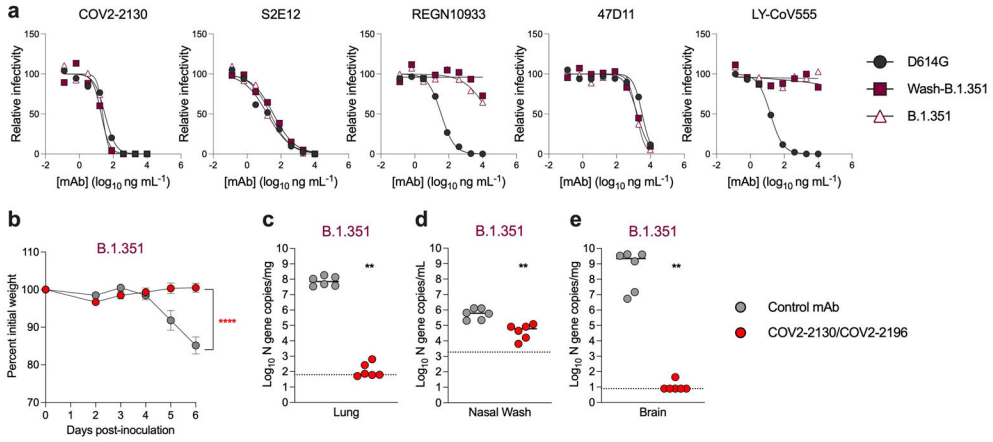

Extended Data Figure 4. Antibody neutralization and protection against a natural B.1.351 isolate.

(**a**) Selected anti-SARS-CoV-2 mAbs (one from each cocktail) were tested for neutralization of infection by WA1/2020 D614G, Wash-B.1.351 or B.1.351 on Vero-TMPRSS2 cells using an FRNT. One representative experiment of two performed in duplicate is shown. (**b-e**) 8-10-week-old female K18-hACE2 transgenic mice received 40 μg (~2 mg/kg) of control mAb or COV2-2130/COV2-2196 by intraperitoneal injection one day before intranasal inoculation with 10^3 FFU of B.1.351. (**b**) Weight change following infection (mean ± SEM; n = 6 mice per group, two experiments; one-way ANOVA with Dunnett's test of area under the curve: ns, not significant, **** $P < 0.0001$). Viral RNA levels in the lung (**c**), nasal wash (**d**), and brain (**e**) (line indicates median; n = 6 mice per group, two experiments; Mann Whitney test: ** $P = 0.002$ (**c-e**)). Dotted line indicates the limit of detection of the assay.

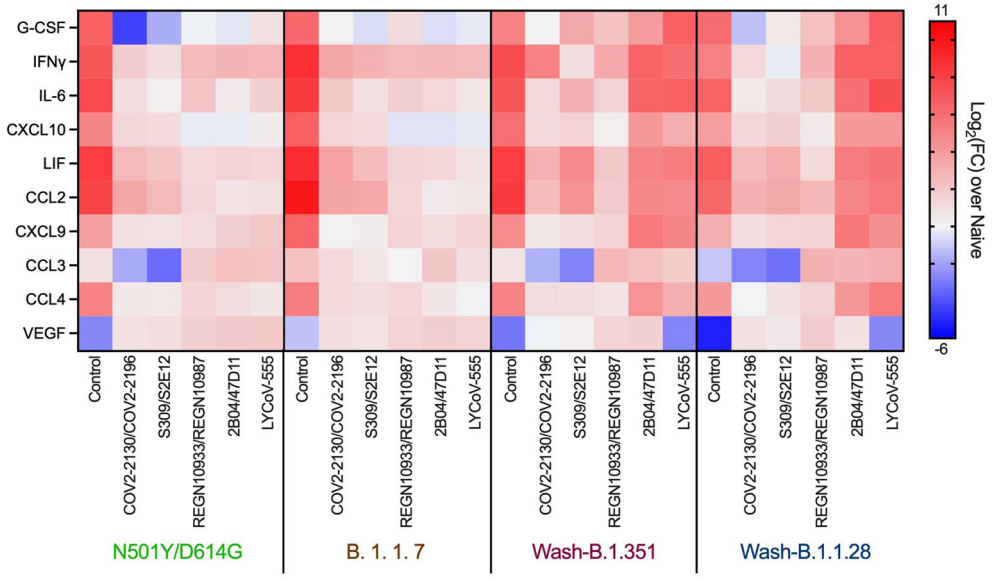

Extended Data Figure 5. Antibody-mediated protection against SARS-CoV-2-induced inflammation.

8-10-week-old female and male K18-hACE2 transgenic mice received 40 μg (~2 mg/kg) of the indicated mAb treatment by intraperitoneal injection one day before intranasal inoculation with 10^3 FFU of the indicated SARS-CoV-2 strain. Heat map of cytokine and chemokine protein expression levels in lung homogenates collected at 6 dpi from the indicated groups. Data are presented as $\log_2$ fold-change over naïve animals. Blue, reduction; red, increase.

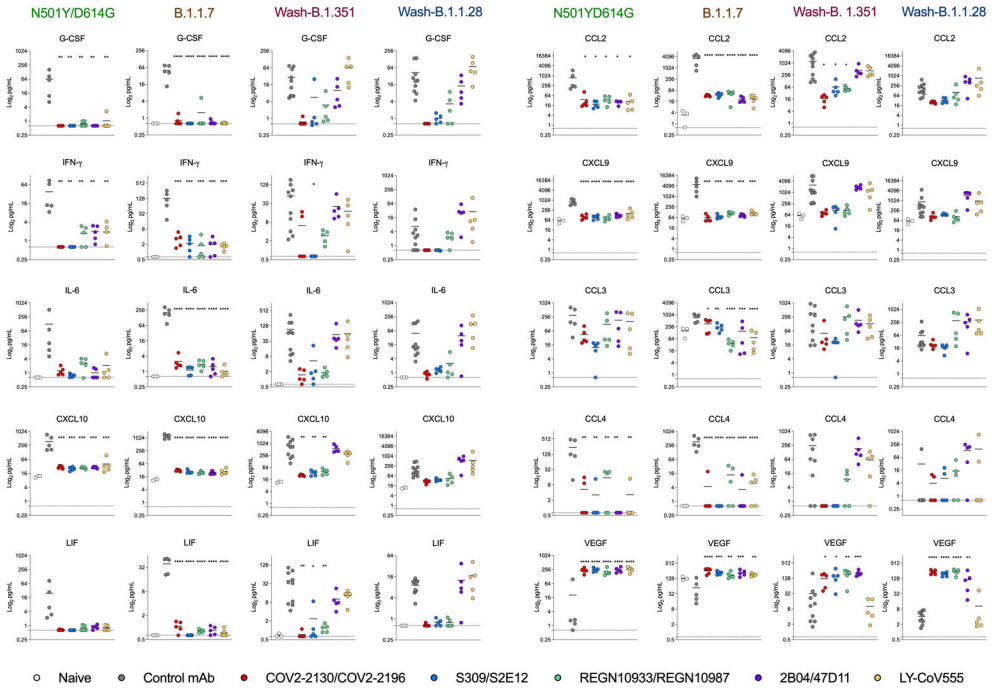

Extended Data Figure 6. Cytokine and chemokine induction following SARS-CoV-2 infection.

Individual plots for cytokine and chemokine protein levels in the lungs of antibody treated K18-hACE2 transgenic mice at 6 dpi after infection with the indicated SARS-CoV-2 strain (line indicates mean; n = 3 naïve, n = 5 for all other groups of B.1.1.7 and N501Y infected mice; n = 3 naïve, 10 control, 5 for all other groups of Wash-B.1.351 and Wash-B.1.1.28 infected mice; one-way ANOVA with Dunnett's test with comparison to control mAb: ns, not significant, **** $P < 0.0001$; all other P values are listed in Supplementary Table S5). Select cytokines and chemokines were used to generate the heat-map in Extended Data Figure 5.

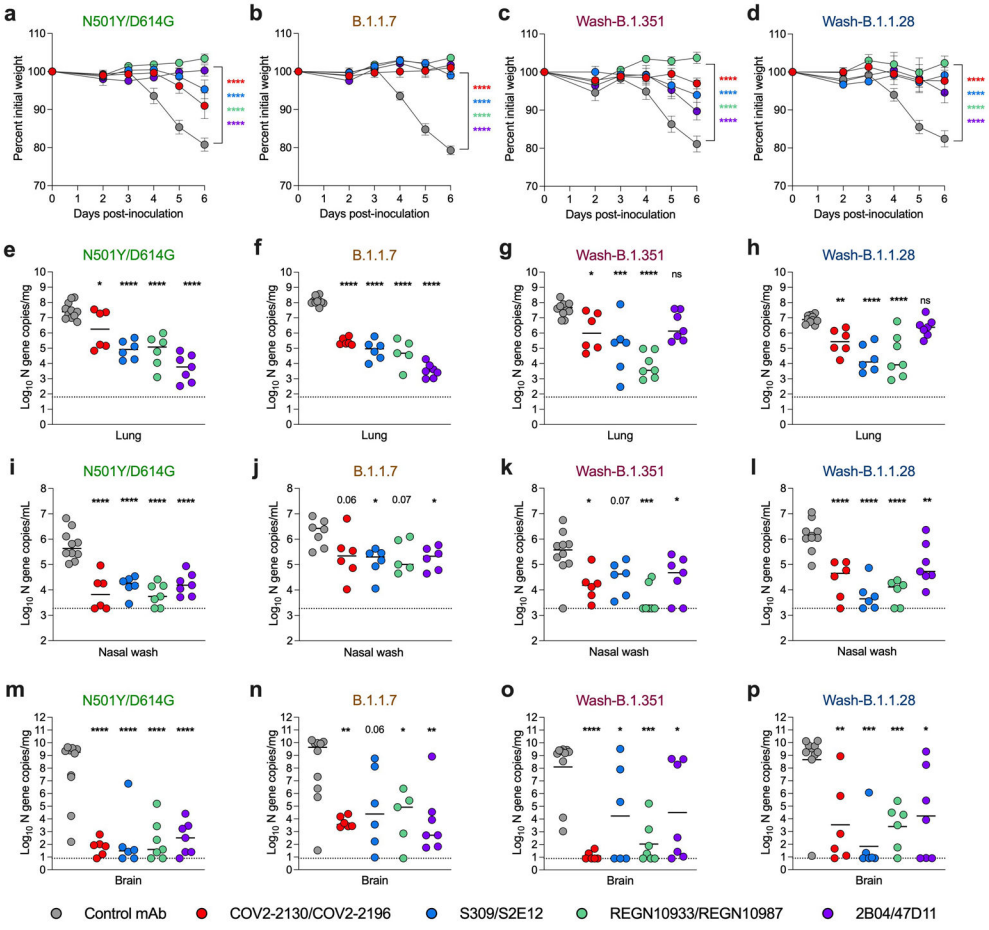

Extended Data Figure 7. Low-dose antibody prophylaxis against SARS-CoV-2 variants in K18-hACE2 mice.

(**a-p**) 8-10-week-old female and male K18-hACE2 transgenic mice received 4 μg (~0.2 mg/kg) of the indicated mAb treatment by intraperitoneal injection one day before intranasal inoculation with 10^3 FFU of the indicated SARS-CoV-2 strain. Tissues were collected at 6 dpi. (**a-d**) Weight change following infection with SARS-CoV-2 (mean ± SEM; in order left to right n = 11, 6, 6, 7, 7 (**a**); n = 10, 6, 6, 5, 7 (**b**); n = 10, 6, 6, 7, 7 (**c-d**) mice per group, two experiments; one-way ANOVA with Dunnett's test of area under the curve with comparison to control mAb: **** $P < 0.0001$). Viral RNA levels in the lung (**e-h**), nasal wash (**i-l**), or brain (**m-p**) were measured (line indicates median; in order from left to right n = 11, 6, 6, 6, 7 (**e**); n = 10, 6, 6, 5, 7 (**f, n**); n = 10, 6, 6, 7, 7 (**g**, **h, i, k, m, and o**); n = 8, 6, 6,

5, 6 (**j**); n = 10, 6, 6, 6, 7 (**l, p**) mice per group, two experiments; one-way ANOVA with Dunnett's test with comparison to isotype control mAb: ns, not significant, **** $P <$ 0.0001); * $P = 0.034$ (**e**); * $P = 0.0422$, *** $P = 0.0004$ (**g**); ** $P = 0.0080$ (**h**); * $P = 0.0209$ (left), 0.0365 (right) (**j**); * $P = 0.0124$ (left), 0.0497 (right), *** $P = 0.0001$ (**k**); ** $P =$ 0.0069 (**l**); ** $P = 0.0087$ (left), 0.0061 (right), * $P = 0.0264$ (**n**); * $P = 0.0378$ (left), 0.0446 (right), *** $P = 0.0004$ (**o**); ** $P = 0.0045$ (left), 0.0035 (right), *** $P = 0.0002$, * $P =$ 0.0107 (**p**)). Dotted line indicates the limit of detection of the assay.

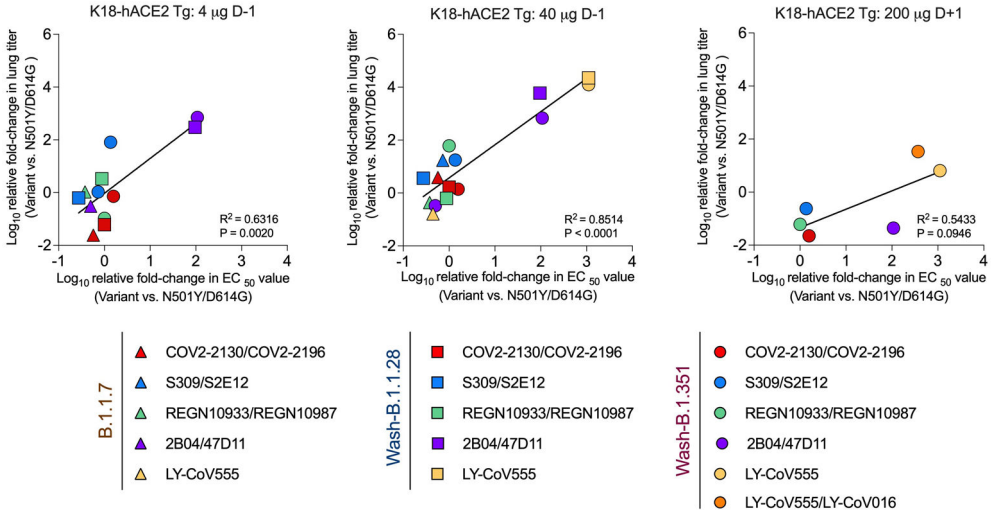

Extended Data Figure 8. ***In vivo*** **correlation of antibody-mediated protection against SARS-CoV-2.**

For each panel, the fold-change in the EC_{50} values of the indicated mAb or mAb cocktails between the N501Y/D614G strain and one or more variants of concern (B.1.1.7, Wash-B.1.351, or Wash-B.1.1.28) were plotted on the x-axis. Next, the fold-change in lung viral RNA titer corresponding to the indicated treatment group (top labels) between the N501Y/D614G strain and one or more variants of concern (B.1.1.7, Wash-B.1.351, or Wash-B.1.1.28) were plotted on the y-axis. Best-fit lines were calculated using a simple linear regression. Two-tailed Pearson correlation was used to calculate R^2 and p values indicated within each panel.

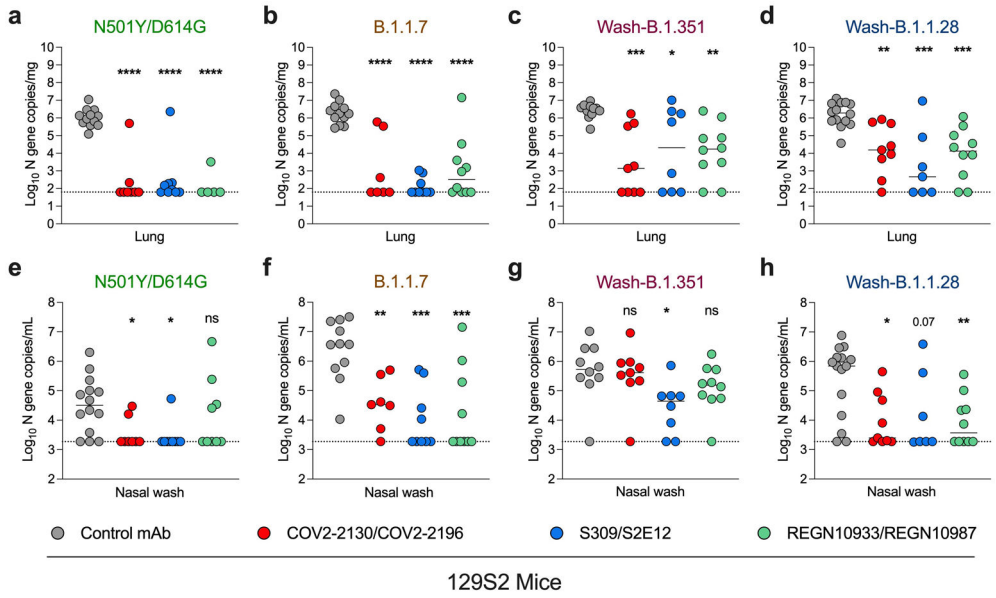

Extended Data Figure 9. Antibody-mediated protection against SARS-CoV-2 variants in 129S2 mice.

(**a-h**) 6-7-week-old female and male immunocompetent 129S2 mice received 40 μg (~ 2 mg/kg) of the indicated mAb treatment by intraperitoneal injection one day before intranasal inoculation with 10^3 FFU of WA1/2020 N501Y/D614G, Wash-B.1.351, or Wash-B.1.1.28 or 10^5 FFU of B.1.1.7. Tissues were collected at 3 dpi. Viral RNA levels in the lung (**a-d**) or nasal washes (**e-h**) were determined (line indicates median; in order left to right n = 12, 8, 6, 5 (**a**); n = 12, 7, 9, 10 (**b**); n = 11, 9, 8, 10 (**c**); n = 14, 9, 6, 5 (**d**); n = 14, 5, 9, 9 (**e**); n = 11, 7, 9, 10 (**f**); n = 10, 9, 8, 10 (**g**); n = 15, 9, 7, 10 (**h**) mice per group, pooled from two to three experiments; one-way ANOVA with Dunnett's test with comparison to control mAb: ns, not significant, *** $P < 0.001$; *** $P = 0.0009$, * $P = 0.0176$, ** $P = 0.0077$ (c); ** $P = 0.0042$, *** $P = 0.0001$ (left), 0.0010 (right) (**d**); * $P = 0.0467$ (left), 0.0188 (right) (**e**); ** $P = 0.0059$, *** $P = 0.0002$ (left), 0.0004 (right) (**f**); * $P = 0.0184$ (**g**), * $P = 0.0129$, ** $P = 0.0090$ (**h**)). Dotted line indicates the limit of detection of the assay.

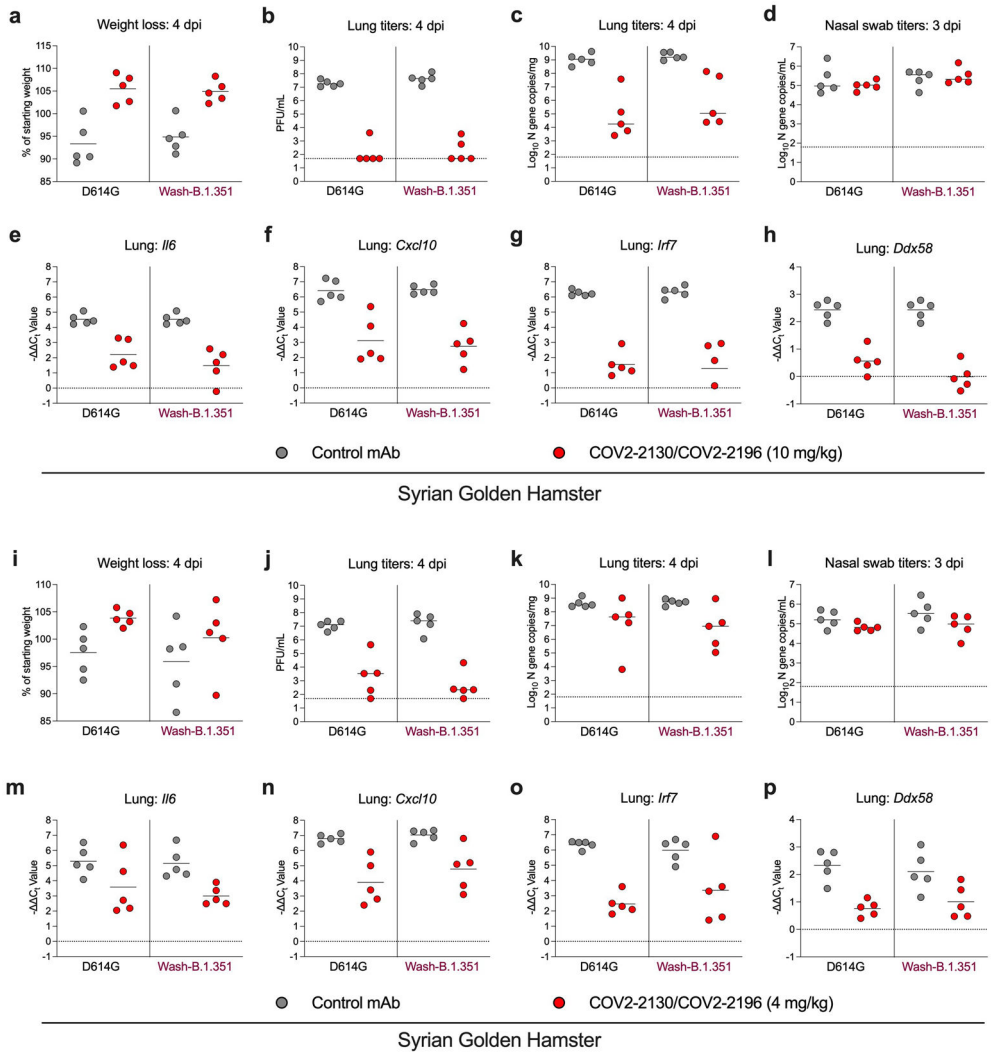

Extended Data Figure 10. COV2-2130/COV2-2196 antibody cocktail protects hamsters against historical and variant SARS-CoV-2 strains.

Six-week-old male Syrian golden hamsters received a single 800 μg (~10 mg/kg) (**a-h**) or 320 μg (~4 mg/kg) dose (**i-p**) of COV2-2130/COV2196 mAb cocktail or control mAb by intraperitoneal injection one day before intranasal inoculation with 5 x 10^5 FFU of WA1/2020 D614G or Wash-B.1.351 viruses. Nasal swabs and lung tissues were collected at 3 and 4 dpi, respectively. (**a**, **i**) Weight change following infection with SARS-CoV-2 (line indicates mean; n = 5 hamsters per group, one experiment). Infectious virus in the lung (**b**, **j**) or viral RNA levels in the lung (**c**, **k**) and nasal swabs (**d**, **l**) were determined (line indicates median; n = 5 animals per group, one experiment). Dotted line indicates the limit of detection of the assay. (**e-h, m-p**) Cytokine and inflammatory gene expression in lung homogenates collected at 6 dpi from indicated groups (line indicates mean; n= 5 hamsters per group). Values were calculated using the $\Delta\Delta C_t$ method compared to a naïve control group. Because data were obtained from a single experiment (even with multiple animals), statistical analysis was not performed.

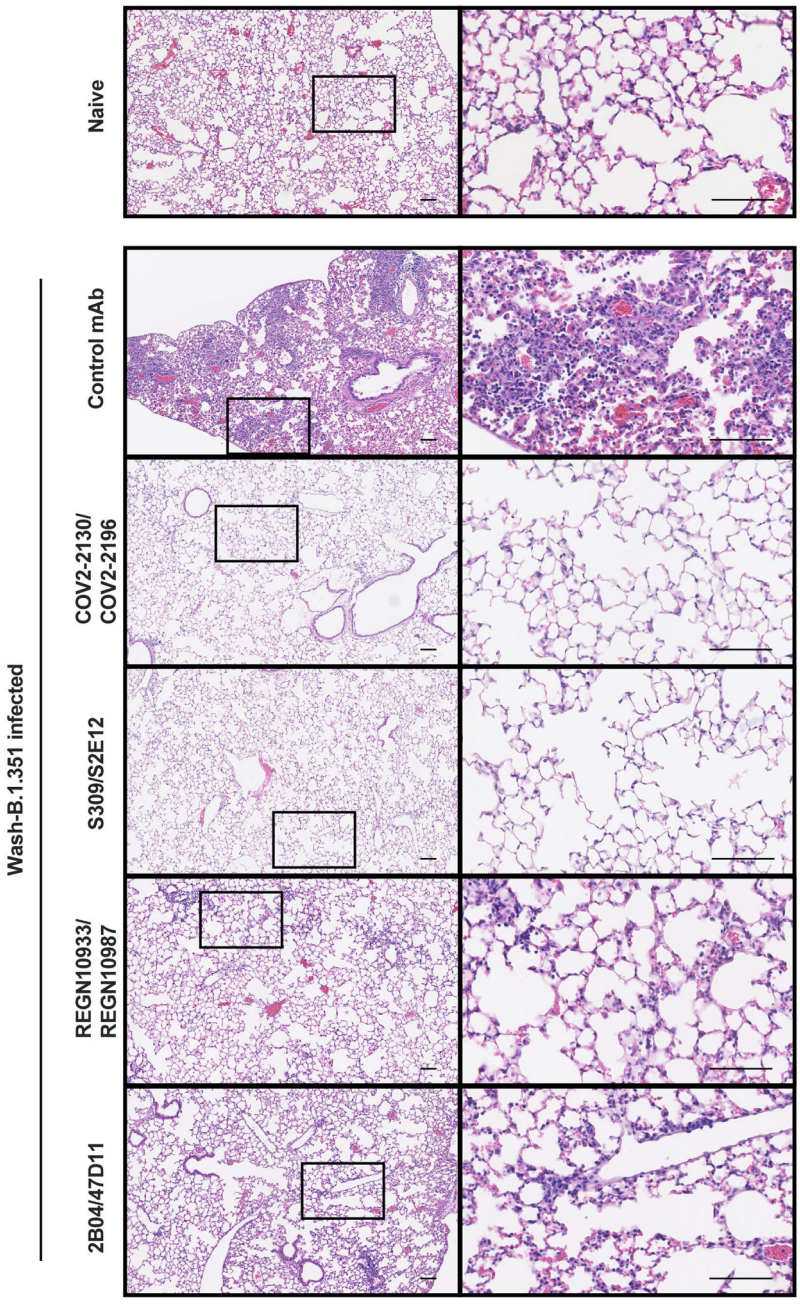

Extended Data Figure 11. Antibody protection against SARS-CoV-2 induced lung pathology.

8-10-week-old female K18-hACE2 transgenic mice received 200 μg (~10 mg/kg) of the indicated mAb treatment or isotype control by intraperitoneal injection one day after intranasal inoculation with 10^3 FFU of Wash-B.1.351 SARS-CoV-2. At 6 dpi, animals were sacrificed and lungs fixed for sectioning prior to staining with hematoxylin and eosin. A lung section from a naïve, uninfected animal is shown (*top panels*) as a reference control. Images show low (left panels for each treatment) and high (right panels for each treatment; boxed region from left) resolution. Scale bars for all images, 100 μm. Representative images from n = 3 mice per group.

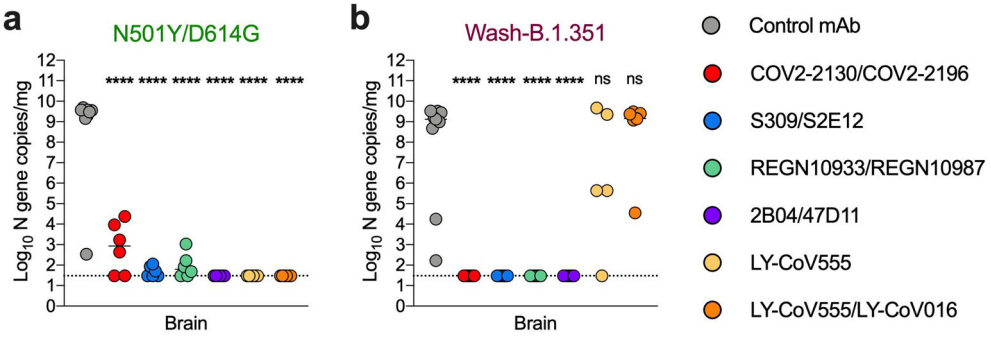

Extended Data Figure 12. Post-exposure antibody therapy against SARS-CoV-2 variants in K18-hACE2 mice.

(**a-b**) 8-10-week-old female and male K18-hACE2 transgenic mice were administered 10^3 FFU of the indicated SARS-CoV-2 strain by intranasal inoculation. One day later, mice received 200 μg (~10 mg/kg) of the indicated mAb treatment by intraperitoneal injection. Tissues were collected at 6 dpi. Viral RNA levels in the brain (**a, b**) (line indicates median; in order left to right n = 9, 6, 6, 6, 6, 6, 6 (**a**); n = 7, 6, 6, 6, 6, 5, 7 (**b**) mice per group, two experiments; one-way ANOVA with Dunnett's test with comparison to control mAb: ns, not significant, **** $P < 0.0001$). Dotted line indicates the limit of detection of the assay.

a

Neutralization on Vero-TMPRSS2 cells	SARS-CoV-2 Viruses								
mAbs EC_{50} (ng/mL)	D614G	N501Y/D614G	B.1.1.7	Wash-B.1.351	Wash-B.1.1.28	B.1.429	B.1.617.1	B.1.526 (S477N)	B.1.526 (E484K)
LY-CoV016	52	290	169	>10,000	>10,000	38	20	9	99
LY-CoV555/LY-CoV016	9	27	11	>10,000	>10,000	63	65	3	261

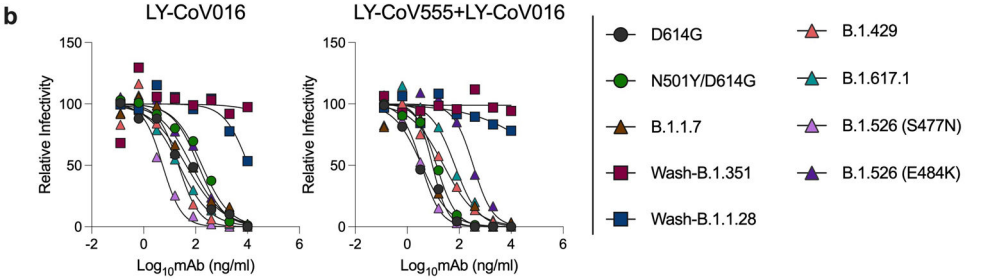

Extended Data Figure 13. Neutralization curves with mAb LY-CoV016 as monotherapy and combination with variant SARS-CoV-2 strains.

Anti-SARS-CoV-2 human mAb LY-CoV016 and combination LY-CoV555/LY-CoV016 (parental mAbs of bamlanivimab and etesevimab, respectively) were tested for inhibition of infection of the indicated SARS-CoV-2 viruses using a FRNT. EC_{50} values (ng/ml) (**a**) and one representative experiment of two performed in duplicate is shown (**b**).

Supplementary Material

Refer to Web version on PubMed Central for supplementary material.

ACKNOWLEDGEMENTS

This study was supported by grants and contracts from NIH (R01 AI157155, U01 AI151810, U01 AI141990, R01 AI118938, 75N93019C00051, HHSN272201400006C, HHSN272201400008C, HHSN75N93019C00074, and HHSN272201400006C), the Children's Discovery Institute (PDII2018702), the Defense Advanced Research Project Agency (HR0011-18-2-0001), the Dolly Parton COVID-19 Research Fund at Vanderbilt University, a grant from Fast Grants, Mercatus Center, George Mason University, and the Future Insight Prize (Merck KGaA; to J.E.C). J.B.C. is supported by a Helen Hay Whitney Foundation postdoctoral fellowship, E.S.W. is supported by F30 AI152327, and S.J.Z. is supported by NIH grant T32 AI095202. P-Y.S. is supported by the Sealy & Smith Foundation, the Kleberg Foundation, the John S. Dunn Foundation, the Amon G. Carter Foundation, the Gilson Longenbaugh Foundation, and the Summerfield Robert Foundation. We thank Rachel Nargi, Robert Carnahan, Tiong Tan, and Lisa Schimanski for assistance and generosity with mAb generation and purification, and Stephen Tahan for some of the deep sequencing analysis. We thank the Pulmonary Morphology Core at Washington University School of Medicine for tissue sectioning and slide imaging.

REFERENCES (MAIN TEXT)

1. Chen RE et al. Resistance of SARS-CoV-2 variants to neutralization by monoclonal and serum-derived polyclonal antibodies. Nat Med, doi:10.1038/s41591-021-01294-w (2021).
2. Wang P et al. Antibody Resistance of SARS-CoV-2 Variants B.1.351 and B.1.1.7. Nature, doi:10.1038/s41586-021-03398-2 (2021).
3. Wang Z et al. mRNA vaccine-elicited antibodies to SARS-CoV-2 and circulating variants. Nature, doi:10.1038/s41586-021-03324-6 (2021).
4. Wibmer CK et al. SARS-CoV-2 501Y.V2 escapes neutralization by South African COVID-19 donor plasma. bioRxiv, doi:10.1101/2021.01.18.427166 (2021).
5. Tada T et al. Neutralization of viruses with European, South African, and United States SARS-CoV-2 variant spike proteins by convalescent sera and BNT162b2 mRNA vaccine-elicited antibodies. bioRxiv, doi:10.1101/2021.02.05.430003 (2021).
6. Xie X et al. Neutralization of SARS-CoV-2 spike 69/70 deletion, E484K and N501Y variants by BNT162b2 vaccine-elicited sera. Nat Med, doi:10.1038/s41591-021-01270-4 (2021).
7. Johnson BA et al. Loss of furin cleavage site attenuates SARS-CoV-2 pathogenesis. Nature, doi:10.1038/s41586-021-03237-4 (2021).
8. Winkler ES et al. SARS-CoV-2 infection of human ACE2-transgenic mice causes severe lung inflammation and impaired function. Nat Immunol 21, 1327–1335, doi:10.1038/s41590-020-0778-2 (2020). [PubMed: 32839612]
9. McCray PB Jr. et al. Lethal infection of K18-hACE2 mice infected with severe acute respiratory syndrome coronavirus. J Virol 81, 813–821, doi:10.1128/jvi.02012-06 (2007). [PubMed: 17079315]
10. Winkler ES et al. Human neutralizing antibodies against SARS-CoV-2 require intact Fc effector functions for optimal therapeutic protection. Cell 184, 1804–1820.e1816, doi:10.1016/j.cell.2021.02.026 (2021). [PubMed: 33691139]
11. Rathnasinghe R et al. The N501Y mutation in SARS-CoV-2 spike leads to morbidity in obese and aged mice and is neutralized by convalescent and post-vaccination human sera. medRxiv : the preprint server for health sciences, doi:10.1101/2021.01.19.21249592 (2021).
12. Gu H et al. Adaptation of SARS-CoV-2 in BALB/c mice for testing vaccine efficacy. Science 369, 1603–1607, doi:10.1126/science.abc4730 (2020). [PubMed: 32732280]
13. Zhou D et al. Robust SARS-CoV-2 infection in nasal turbinates after treatment with systemic neutralizing antibodies. Cell Host Microbe, doi:10.1016/j.chom.2021.02.019 (2021).
14. Andreano E et al. Extremely potent human monoclonal antibodies from COVID-19 convalescent patients. Cell 184, 1821–1835.e1816, doi:10.1016/j.cell.2021.02.035 (2021). [PubMed: 33667349]
15. Schäfer A et al. Antibody potency, effector function, and combinations in protection and therapy for SARS-CoV-2 infection in vivo. J Exp Med 218, doi:10.1084/jem.20201993 (2021).
16. Bournazos S, Corti D, Virgin HW & Ravetch JV Fc-optimized antibodies elicit CD8 immunity to viral respiratory infection. Nature, doi:10.1038/s41586-020-2838-z (2020).

17. Cobey S, Larremore DB, Grad YH & Lipsitch M Concerns about SARS-CoV-2 evolution should not hold back efforts to expand vaccination. Nat Rev Immunol, 1–6, doi:10.1038/s41577-021-00544-9 (2021). [PubMed: 33303954]
18. Shen X et al. Neutralization of SARS-CoV-2 Variants B.1.429 and B.1.351. N Engl J Med, doi:10.1056/NEJMc2103740 (2021).
19. McCallum M et al. SARS-CoV-2 immune evasion by variant B.1.427/B.1.429. bioRxiv, doi:10.1101/2021.03.31.437925 (2021).
20. Lundgren JD et al. A Neutralizing Monoclonal Antibody for Hospitalized Patients with Covid-19. N Engl J Med 384, 905–914, doi:10.1056/NEJMoa2033130 (2021). [PubMed: 33356051]
21. Reynolds HY Immunoglobulin G and its function in the human respiratory tract. Mayo Clinic proceedings 63, 161–174, doi:10.1016/s0025-6196(12)64949-0 (1988). [PubMed: 3276975]
22. Borrok MJ et al. Enhancing IgG distribution to lung mucosal tissue improves protective effect of anti-Pseudomonas aeruginosa antibodies. JCI insight 3, doi:10.1172/jci.insight.97844 (2018).
23. Gottlieb RL et al. Effect of Bamlanivimab as Monotherapy or in Combination With Etesevimab on Viral Load in Patients With Mild to Moderate COVID-19: A Randomized Clinical Trial. Jama 325, 632–644, doi:10.1001/jama.2021.0202 (2021). [PubMed: 33475701]
24. Wang P et al. Increased resistance of SARS-CoV-2 variant P.1 to antibody neutralization. Cell Host Microbe 29, 747–751.e744, doi:10.1016/j.chom.2021.04.007 (2021). [PubMed: 33887205]
25. Starr TN, Greaney AJ, Dingens AS & Bloom JD Complete map of SARS-CoV-2 RBD mutations that escape the monoclonal antibody LY-CoV555 and its cocktail with LY-CoV016. Cell reports. Medicine, 100255, doi:10.1016/j.xcrm.2021.100255 (2021). [PubMed: 33842902]
26. Schmitz AJ et al. A public vaccine-induced human antibody protects against SARS-CoV-2 and emerging variants. bioRxiv, doi:10.1101/2021.03.24.436864 (2021).
27. Tian F et al. Mutation N501Y in RBD of Spike Protein Strengthens the Interaction between COVID-19 and its Receptor ACE2. BioRxiv, doi:10.1101/2021.02.14.431117 (2021).
28. Graham C et al. Neutralization potency of monoclonal antibodies recognizing dominant and subdominant epitopes on SARS-CoV-2 Spike is impacted by the B.1.1.7 variant. Immunity, doi:10.1016/j.immuni.2021.03.023 (2021).
29. Rees-Spear C et al. The effect of spike mutations on SARS-CoV-2 neutralization. Cell Rep 34, 108890, doi:10.1016/j.celrep.2021.108890 (2021). [PubMed: 33713594]
30. Zhou D et al. Evidence of escape of SARS-CoV-2 variant B.1.351 from natural and vaccine-induced sera. Cell, doi:10.1016/j.cell.2021.02.037 (2021).
31. Baum A et al. Antibody cocktail to SARS-CoV-2 spike protein prevents rapid mutational escape seen with individual antibodies. Science, doi:10.1126/science.abd0831 (2020).

REFERENCES (METHODS AND SUPPLEMENTAL TABLES)

32. Goddard TD et al. UCSF ChimeraX: Meeting modern challenges in visualization and analysis. Protein Sci 27, 14–25, doi:10.1002/pro.3235 (2018). [PubMed: 28710774]
33. Zang R et al. TMPRSS2 and TMPRSS4 promote SARS-CoV-2 infection of human small intestinal enterocytes. Sci Immunol 5, doi:10.1126/sciimmunol.abc3582 (2020).
34. Plante JA et al. Spike mutation D614G alters SARS-CoV-2 fitness. Nature, doi:10.1038/s41586-020-2895-3 (2020).
35. Edara V-V et al. Infection and vaccine-induced neutralizing antibody responses to the SARS-CoV-2 B.1.617.1 variant. bioRxiv, 2021.2005.2009.443299, doi:10.1101/2021.05.09.443299 (2021).
36. Zost SJ et al. Rapid isolation and profiling of a diverse panel of human monoclonal antibodies targeting the SARS-CoV-2 spike protein. Nat Med 26, 1422–1427, doi:10.1038/s41591-020-0998-x (2020). [PubMed: 32651581]
37. Pinto D et al. Cross-neutralization of SARS-CoV-2 by a human monoclonal SARS-CoV antibody. Nature 583, 290–295, doi:10.1038/s41586-020-2349-y (2020). [PubMed: 32422645]

38. Tortorici MA et al. Ultrapotent human antibodies protect against SARS-CoV-2 challenge via multiple mechanisms. Science 370, 950–957, doi:10.1126/science.abe3354 (2020). [PubMed: 32972994]

39. Alsoussi WB et al. A Potently Neutralizing Antibody Protects Mice against SARS-CoV-2 Infection. J Immunol, doi:10.4049/jimmunol.2000583 (2020).

40. Baum A et al. REGN-COV2 antibodies prevent and treat SARS-CoV-2 infection in rhesus macaques and hamsters. Science, doi:10.1126/science.abe2402 (2020).

41. Jones BE et al. LY-CoV555, a rapidly isolated potent neutralizing antibody, provides protection in a non-human primate model of SARS-CoV-2 infection. bioRxiv, doi:10.1101/2020.09.30.318972 (2020).

42. Shi R et al. A human neutralizing antibody targets the receptor-binding site of SARS-CoV-2. Nature 584, 120–124, doi:10.1038/s41586-020-2381-y (2020). [PubMed: 32454512]

43. Liu Z et al. Identification of SARS-CoV-2 spike mutations that attenuate monoclonal and serum antibody neutralization. Cell Host Microbe 29, 477–488.e474, doi:10.1016/j.chom.2021.01.014 (2021). [PubMed: 33535027]

44. Case JB, Bailey AL, Kim AS, Chen RE & Diamond MS Growth, detection, quantification, and inactivation of SARS-CoV-2. Virology 548, 39–48, doi:10.1016/j.virol.2020.05.015 (2020). [PubMed: 32838945]

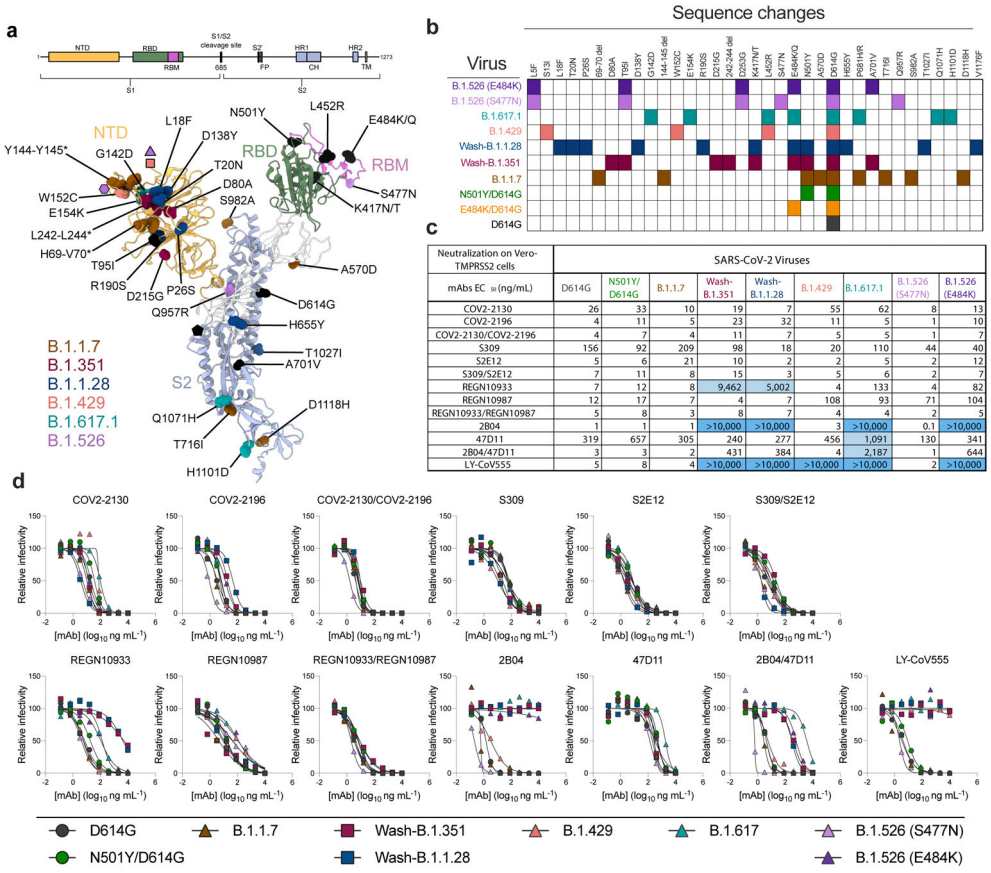

Figure 1. Neutralization of SARS-CoV-2 variant strains by clinically relevant mAbs.

(**a-b**) SARS-CoV-2 variant substitutions mapped onto the structure of the spike protein. Schematic layout of the spike protein monomer is depicted at the top. Structure of spike monomer (PDB: 7C2L with RBD from PDB: 6W41) is depicted as a cartoon, with NTD, RBD, RBM, and S2 colored orange, green, magenta, and light blue, respectively. Substitutions for each variant are shown as spheres and colored according to the legend. Substitutions shown in black are shared between multiple variants. Purple triangle, pink square, purple pentagon, and black hexagon represent approximate locations of L5, S13, D253 and P681 respectively, which were not modeled in the original structures. (**a**) Structural figure generated using UCSF ChimeraX[32]. (**b**) Viruses used with indicated colored mutations in the spike protein. (**c**) Summary of EC_{50} values (ng/mL) of neutralization of SARS-CoV-2 viruses performed in Vero-TMPRSS2 cells. Blue shading of cells indicates a partial (EC_{50} > 1,000 ng/mL) or complete (EC_{50} > 10,000 ng/mL) loss of neutralizing activity. (**d**) Neutralization curves comparing the sensitivity of SARS-CoV-2 strains to the indicated individual or combinations of mAbs. Data are representative of two to five experiments, each performed in technical duplicate.

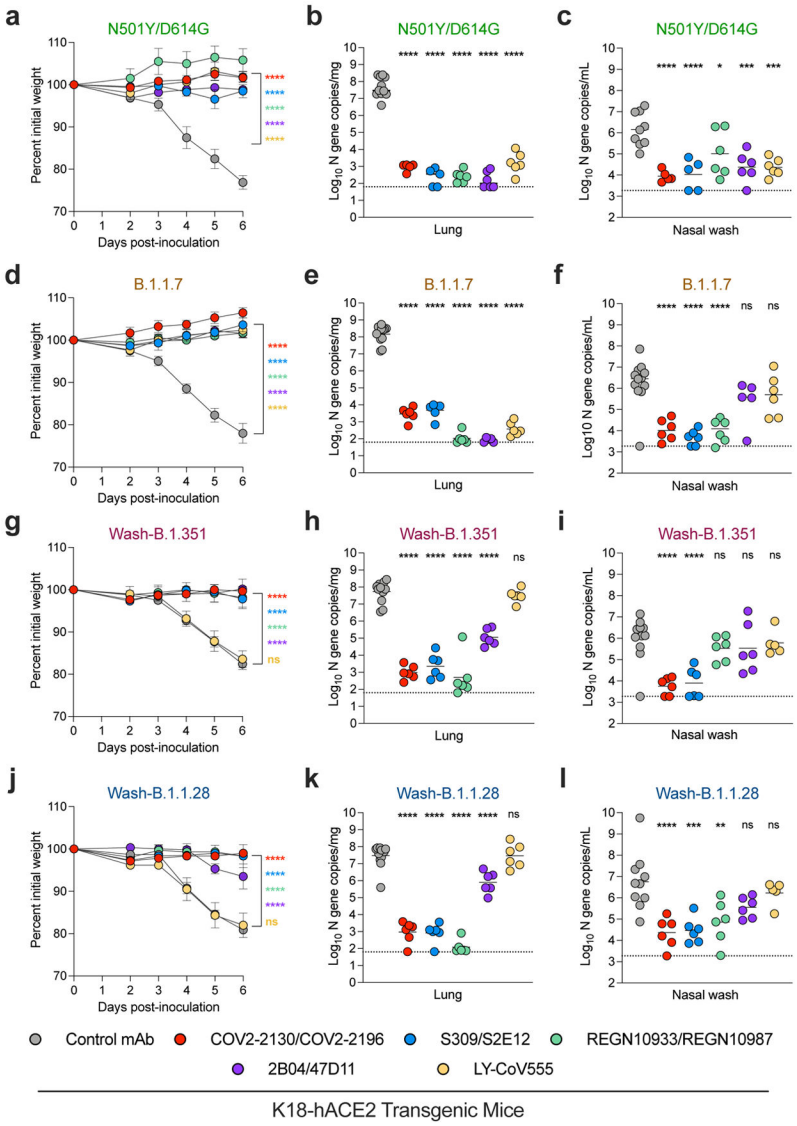

Figure 2. Antibody prophylaxis against SARS-CoV-2 variants in K18-hACE2 mice.

(**a-l**) 8-10-week-old female and male K18-hACE2 transgenic mice received 40 μg (~2 mg/kg) of the indicated mAb treatment by intraperitoneal injection one day before intranasal inoculation with 10^3 FFU of the indicated SARS-CoV-2 strain. Tissues were collected at 6 dpi. (**a**, **d**, **g**, **j**) Weight change following infection with SARS-CoV-2 (mean ± SEM; n = 6-12 mice per group, two experiments; one-way ANOVA with Dunnett's test of area under the curve: ns, not significant, **** $P < 0.0001$). Viral RNA levels in the lung (**b**, **e**, **h**, **k**) and nasal washes (**c**, **f**, **i**, **l**) were measured (line indicates median; in order left to right n = 9, 6, 7, 6, 6, 6 (**a**); n = 11, 5, 5, 6, 6, 6 (**b**); n = 9, 5, 5, 6, 6, 6 (**c**); n = 12, 6, 6, 6, 5, 6 (**d-f**); n = 12, 6, 6, 6, 6, 6 (**g-h, and j-k**); n = 12, 6, 6, 6, 6, 5 (**i**); n = 10, 6, 6, 6, 6, 5 (**l**) mice per group, two experiments; one-way ANOVA with Dunnett's test with comparison to control mAb: ns, not significant, **** $P < 0.0001$; * $P = 0.026$ (**c**); ** $P = 0.0016$, *** $P = 0.0002$ (**l**)). Dotted line indicates the limit of detection of the assay.

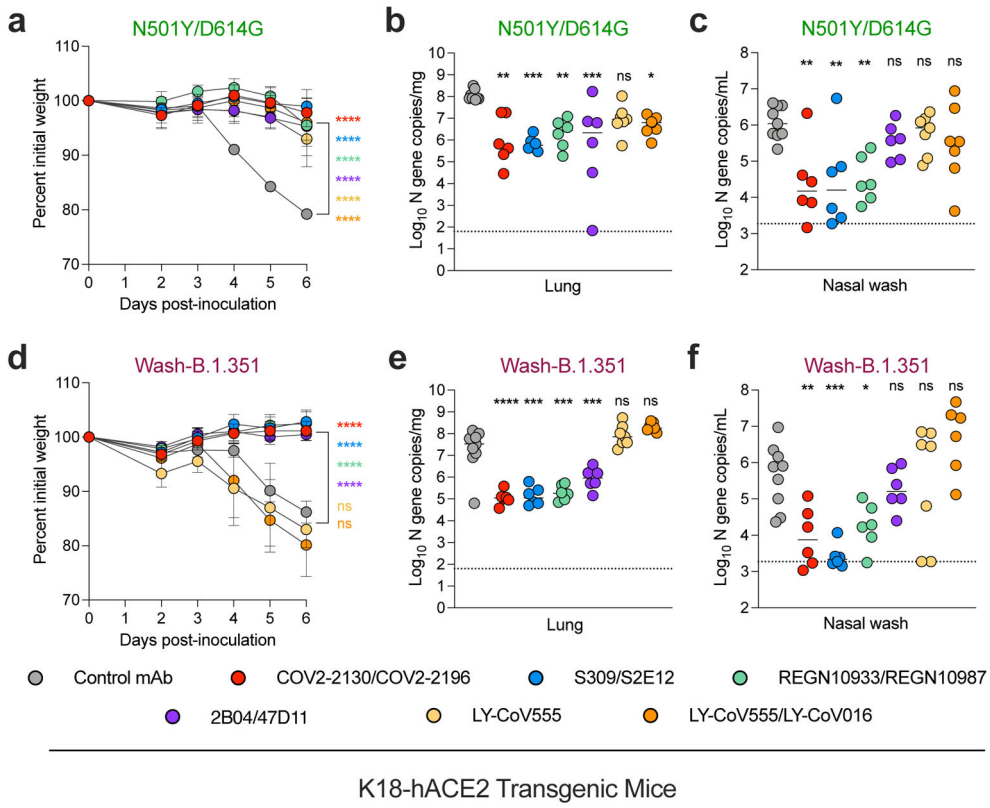

Figure 3. Post-exposure antibody therapy against SARS-CoV-2 variants in K18-hACE2 mice.

(**a-f**) 8-10-week-old female and male K18-hACE2 transgenic mice were administered 10^3 FFU of the indicated SARS-CoV-2 strain by intranasal inoculation. One day later, mice received 200 μg (~10 mg/kg) of the indicated mAb treatment by intraperitoneal injection. Tissues were collected at 6 dpi. (**a**, **d**) Weight change following infection with SARS-CoV-2 (mean ± SEM; in order left to right n = 15, 6, 6, 6, 6, 7, 7 (**a, d**) mice per group, two experiments; one-way ANOVA with Dunnett's test of area under the curve: ns, not significant, **** $P < 0.0001$). Viral RNA levels in the lung (**b**, **e**) and nasal wash (**c**, **f**) (line indicates median; in order left to right n = 7, 6, 6, 6, 6, 7, 7 (**b**); n = 9, 6, 6, 6, 6, 7, 7 (**c, e, and f**) mice per group, two experiments; one-way ANOVA with Dunnett's test with comparison to control mAb: ns, not significant, **** $P < 0.0001$; ** $P = 0.0014$ (left), 0.0088 (right), *** $P = 0.0007$ (left), 0.0003 (right) (**b**); ** $P = 0.0026$ (left), 0.0041 (middle), 0.0049 (right) (**c**); ** $P = 0.0049$, *** $P = 0.0004$ (**e**); ** $P = 0.0094$, *** $P = 0.0005$, * $P = 0.0442$ (**f**). Dotted line indicates the limit of detection of the assay.